A 26 GHz rectenna based on a solar cell antenna for internet of things applications

Chokri Baccouch[1], Saleh Omar[2], Belgacem C. Rhaimi[2]
[1]SYS'COM Laboratory LR99ES21, National Engineering School of Tunis, Tunis El Manar University, Tunis, Tunisia
[2]MACS Laboratory: Modeling, Analysis and Control of Systems LR16ES22, National Engineering School of Gabes, University of Gabes, Gabes, Tunisia

Article Info

Article history:

Received Jan 18, 2024
Revised May 20, 2024
Accepted Jun 4, 2024

Keywords:

5G
Drones
Energy harvesting
internet of things
Patch antenna
Solar cell
Wireless communications

ABSTRACT

This paper presents a new rectenna system that combine a patch antenna with a solar cell to capture energy from both radio frequency (RF) signals and sunlight. The patch antenna collects RF signals, while the solar cell converts sunlight into electricity. This integration offers a sustainable energy solution for internet of things (IoT) sensors or drones. The antenna's performance at 26 GHz demonstrates impressive metrics, including a -68 dB S11 reflection, 700 MHz bandwidth, 6.25 dBi gain, 49.8 Ω impedance, and 42.25% RF-DC conversion efficiency. The "solar rectenna" integrates both technologies, driving technological advancement and fostering sustainability in wireless communication.

Corresponding Author:

Chokri Baccouch
SYS'COM Laboratory LR99ES21, National Engineering School of Tunis, Tunis El Manar University
Rommana 1068, Tunis, Tunisia
Email: chokri.baccouch13@gmail.com

1. INTRODUCTION

The advent of Industry 4.0, initiated by the fourth industrial revolution in 2011, symbolizes the fusion of technologies across physical, digital, and biological domains. This revolution heralds significant progress in fields such as robotics, artificial intelligent (AI), blockchain, nanotechnology, quantum computing, biotechnology, internet of things (IoT), 3D printing, and advanced mobile communications. Notably, it catalyzes the emergence of autonomous vehicles like drones and drives extensive technology integration into manufacturing, giving rise to the "smart factory" concept [1]–[3]. Concurrently, the communications and information technology sector rapidly evolve to deliver cutting-edge solutions for advanced communication services, adhering to international standards. Utilizing wireless communication, smart antennas, sensors, and aerial communication systems, including satellites and drones, facilitates the deployment of smart digital applications and services. This evolution, particularly in the 5G era, enriches daily lives and fosters connections in modern smart societies [4]–[6].

The innovative technology of 5G in wireless communication promises exceptional service marked by high speed, versatility, and user-friendliness [7]. This advancement is poised to foster a "sustainable communications community" where mobile devices play a pivotal role in enhancing daily lives. As data rates and connected devices on the 5G network increase, deploying advanced technologies like massive multiple-input and multiple-output (MIMO) systems becomes crucial. Notably, 5G MIMO antennas typically operate at higher frequencies for enhanced data rates, albeit posing challenges such as shorter range and covering smaller geographic cells, emphasizing the need for careful trade-offs.

The rise of IoT relies increasingly on wireless capabilities, supplanting traditional wired systems. Adoption of wireless communication, alongside advanced antennas like 5G MIMO, has markedly hastened IoT development and deployment. Experts predict widespread adoption across sectors like healthcare (for remote robotic operations) and smart infrastructure facilitating communication between city traffic lights. Various smart IoT applications have emerged, revolutionizing sectors such as insurance, healthcare, agriculture, and monitoring [8]–[13]. Figure 1 illustrates a typical network infrastructure for 5G IoT applications.

This paper proposes the design of 5G printed antenna tailored for millimeter wave bands, specifically for use in the satellite-routed sensor system (SRSS) to support IoT applications. It offers a novel approach compared to previous studies. The subsequent sections of this paper are organized as follows: section 2 details the design and implementation procedures for the proposed antenna. Section 3 covers the simulation results, while section 4 presents the proof of concept. Concluding remarks are offered in section 5.

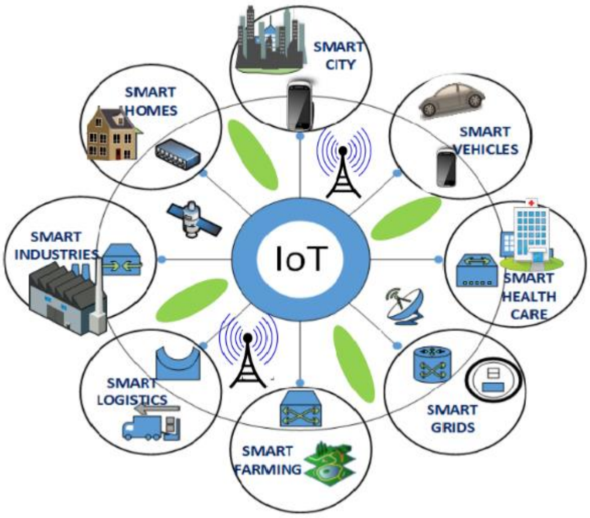

Figure 1. Internet of things: connecting "anything, anyone, anytime, anyplace" [5]

2. RELATED WORKS

In a prior investigation [14], a single-port dual-band antenna was devised for 2.45 GHz WLAN applications, incorporating solar cells into its architecture. Thirty solar cells were utilized, serving both as guides and forming the primary radiation structure in the low and high bands, respectively. To achieve dual-frequency performance, microstrip and slot antennas were seamlessly integrated into compact structures, exploiting various multiple resonance modes. Measurement outcomes indicated that the lower band covered a range of 2.27-2.5 GHz with an omnidirectional radiation pattern, while the higher band exhibited a gain range of 4.8-6.9 dBi.

In another study [15], a multipoint feed patch antenna was developed, incorporating an aperture linked to a solar cell aimed at powering low-consumption wireless sensors. Strategically placing the solar cells on the structure served both as heat sinks and enhanced overall integration. The antenna achieved broadband performance through a multipoint power structure. Simulations and measurements showed consistent results, indicating that the antenna, with dimensions of $1.31\lambda_0 \times 1.31\lambda_0 \times 0.06\lambda_0$ (where λ_0 denotes the wavelength in free space at the center frequency), maintained a stable gain of 9.47 from 4.8 to 5 GHz for 5G communications and a peak gain of 10.85 dBi across the operating frequency band.

In a separate study [16], a compact photovoltaic cell integrated with an antenna was proposed for IoT applications. The design features a gallium arsenide photovoltaic cell with a hexagonal slot and trapezoidal disturbances in its active area. The lower contacts of the photovoltaic cell also serve as the ground plane for the antenna. An AC blocking circuit and chip inductor are integrated to prevent RF current flow into the photovoltaic cells. This configuration allows the device to function as both a photovoltaic cell and an antenna. The GaAs photovoltaic cell exhibited a power conversion efficiency of 13.25% without an anti-reflective coating, with measured open circuit voltage at 0.963 V, 21.00 mA/cm^2 of short circuit current density, and 65.52% fill factor. The complete structure's dimensions are 31.4×33×0.639 mm, and the antenna operates in the frequency range of 2.14 to 2.94 GHz, with a gain of 2.8 dBi at 2.45 GHz.

In the study described in [17], a compact antenna with thin slots integrated with photovoltaic cells is proposed. The photovoltaic cell consists of a gallium arsenide substrate with upper and lower metallic contacts, where the lower contact acts as the ground plane. Grooves are etched for resonance, and a second substrate beneath the ground plane features 50 Ω microstrip lines to excite the slot. Chip inductors serve as RF chokes in AC blocking circuits to prevent RF current leakage to the photovoltaic cells. This design enables the antenna to function as both a photovoltaic cell and an antenna. With dimensions of 25×31.75×0.893 mm ($0.48\lambda_0 \times 0.61\lambda_0 \times 0.017\lambda_0$, 5.77 GHz), it is suitable for effective use in IoT devices.

In study [18], a portable system is developed to harvest microwave energy by integrating dual-band microstrip antennas. These antennas are implemented on thin multilayers within the package, with denim cotton used for constructing the rectifier and associated circuitry. The performance of the antennas is evaluated under mechanical bending conditions, showing consistent power conversion efficiency. The voltage doubling efficiency is tested by varying the RF power level from -30 to 10 dBm. The conversion efficiencies at 1.85 and 2.45 GHz, with a 7.5 kΩ load, are recorded as 58% and 43%, respectively.

In study [19], a coplanar patch antenna integrated with a solar cell is designed for operation in the 2.4 GHz frequency band. The simulation results are validated through characterization and prototyping. The achieved gain is 4.13 dBi with a bandwidth of 15.14% and an efficiency of 87.1% at 2.45 GHz.

Table 1 summarizes the conclusions of related research in comparison to your proposed antenna design, describing different related works with their parameters such as antenna type, frequency (GHz), antenna dimensions, substrate type, gain, and probable application.

Table 1. Related research windup against our proposed antenna design

Ref. No.	Antenna type	Freq (GHz)	Antenna size (mm)	Substrate	Gain (dBi)	Probable Applications
[16]	Subsolar	2.27-2.50	50 x50	NR	4.8 -6.9	WLAN applications
[17]	Supersolar	2.14-2.94	31.4x33	gallium arsenide	2.8	IoT applications
[20]	Supersolar	5.77	25-31.75	gallium arsenide	NR	IoT devices
[21]	Subsolar	4.8–5	40x40	NR	9.47–10.85	5G communications
[22]	Super solar	2.45	18x15	NR	4.13	Wi-Fi
[23]	Super solar	8.51-9.10	26.8x24.1	glass substrates	NR	NR
Work	Super solar	26	2.4 × 1.7	FR4	6.25	SRSS and drones' applications

3. SOLAR RECTENNA FOR SATELLITE BASED IOT SERVICES

This study shifts its focus to a data collection method employing the SRSS, recognized as advanced technology for efficient data retrieval from wireless sensor terminals. Within SRSS, as illustrated in Figure 2, satellites transmit data from terminals situated in urban or challenging environments to a ground station for management. Satellite networks demonstrate proficiency in facilitating simultaneous communication, enabling multiple sensors to access the network concurrently [24]–[26].

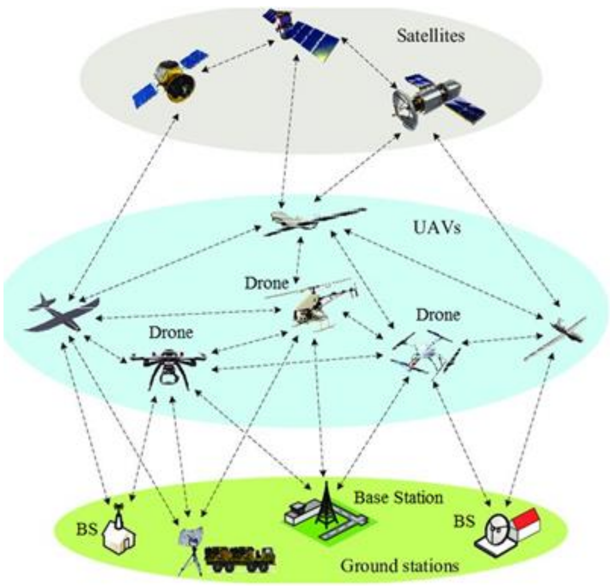

Figure 2. An example of an SRSS used for facilitating the IoT

In our study, the solar rectenna system we propose is designed to harness both electromagnetic energy and solar waves for wireless communications with SRSS. It operates by capturing energy from these sources using a receiving optical antenna and converting it into direct current (DC) via a rectifier circuit, as depicted in Figure 3. The process begins with the antenna capturing electromagnetic and solar waves, which are then directed to a conversion circuit [27], [28]. This circuit, incorporating one or more diodes, efficiently converts RF energy into continuous electrical power. The generated power is then delivered to a resistive load (RL), as shown in Figure 4.

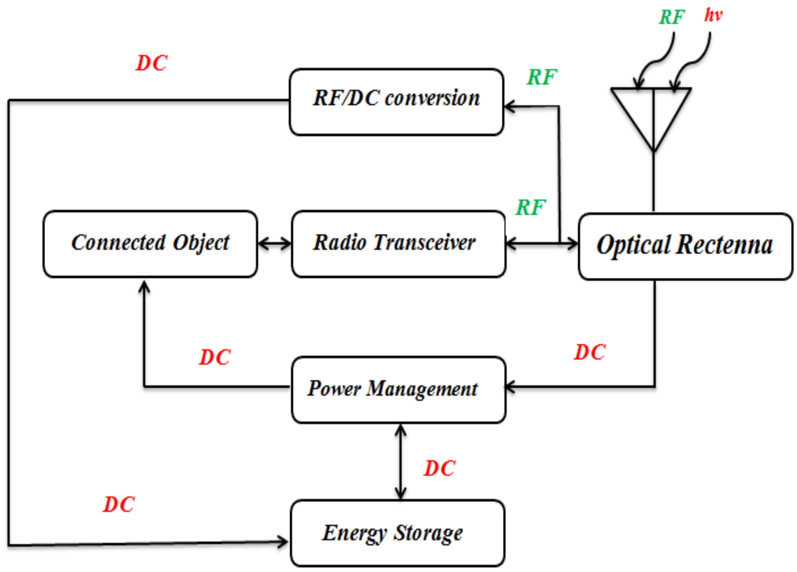

Figure 3. Optical rectenna architecture

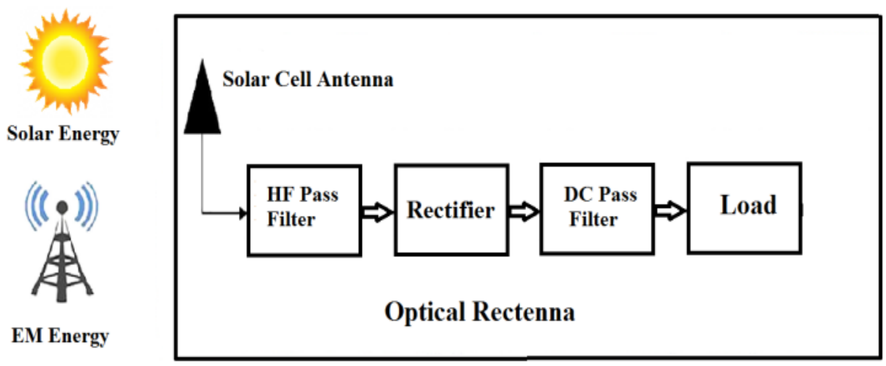

Figure 4. Global structure of an optical rectenna system

4. PROPOSED ANTENNA DESIGN

This section centers on the design of the proposed 5G antenna, a single-patch printed antenna known for its compact size and resonant frequency of 26 GHz. Figure 5 depicts the antenna's structure and dimensions, highlighting the partial ground plane on the antenna substrate. The proposed antenna, operating at 26 GHz, features a "Yagi" design encased within a rectangular element alongside a partial ground plane. This configuration offers several notable attributes in terms of bandwidth, impedance, gain, and polarization. We assess the performance of the proposed antenna using various performance metrics, offering a comprehensive comparison between the measured and simulated results. To validate the experiment, we fabricated a prototype of the antenna on an FR-4 substrate, as illustrated in Figure 6. Table 2 displays the dimensions of the antenna at 26 GHz.

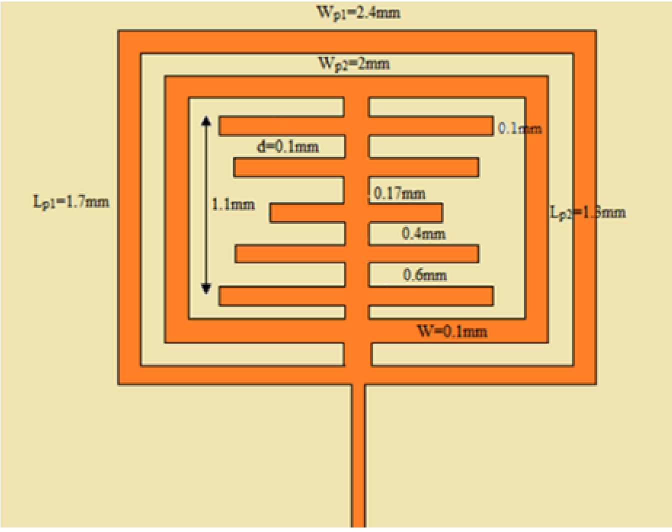

Figure 5. Proposed antenna at 26 GHz

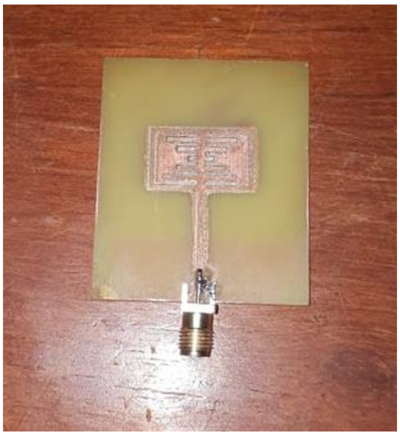

Figure 6. Fabricated antenna at 26 GHz

Table 2. Antenna dimensions

Antenna	Patch width W_p (mm)	Patch length L_p (mm)	Ground plane length LG (mm)	Ground plane width WG (mm)	Feed width W_F (mm)	Feed length L_F (mm)	Substrate width Ws (mm)	Substrate length Ls (mm)
26 GHz	2.4	1.7	1.2	6.9	0.15	2.25	12.7	10.4

5. RESULTS AND DISCUSSION

This section presents visualized results of the proposed antenna structure alongside detailed discussions. Figures 7 to 14 display the simulation results of S11 value, 3D directivity diagram, voltage standing wave ratio (VSWR), conversion circuit, and conversion efficiency. It is crucial to note that the simulation aims to identify both intrinsic parameters (S-parameters, bandwidth in dB, and bandwidth in Hz) and extrinsic characteristics (gain, directivity, and radiation model).

5.1. S-parameters

Figure 7 presents the comparison between the measured and simulated reflection coefficients of the proposed antenna. The antenna shows resonance at 26 GHz, with a notable bandwidth of approximately 700 MHz from 25.7 to 26.4 GHz. Importantly, the antenna exhibits robust performance across the entire 26 GHz frequency band allocated for 5G millimeter wave communications. Overall, there is a strong agreement between the simulation and measurement results, acknowledging that minor discrepancies may arise due to manufacturing variations and inaccuracies in measurement equipment.

5.2. Radiation pattern

Figures 8 and 9 display the simulated 3D and 2D radiation patterns, respectively. These illustrations reveal concentrated radiation predominantly at the antenna's top. The 2D radiation pattern offers insights into the lobes' distribution, particularly in the vertical and horizontal planes. Notably, a larger lobe is noticeable in both patterns, particularly at angles of phi = 0° and phi = 90°.

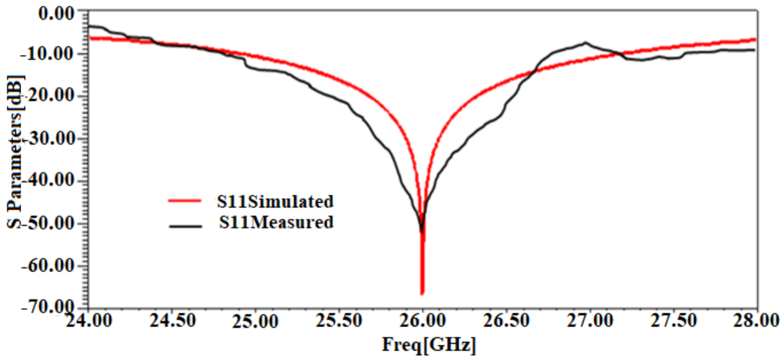

Figure 7. Reflection coefficient of antenna at 26 GHz

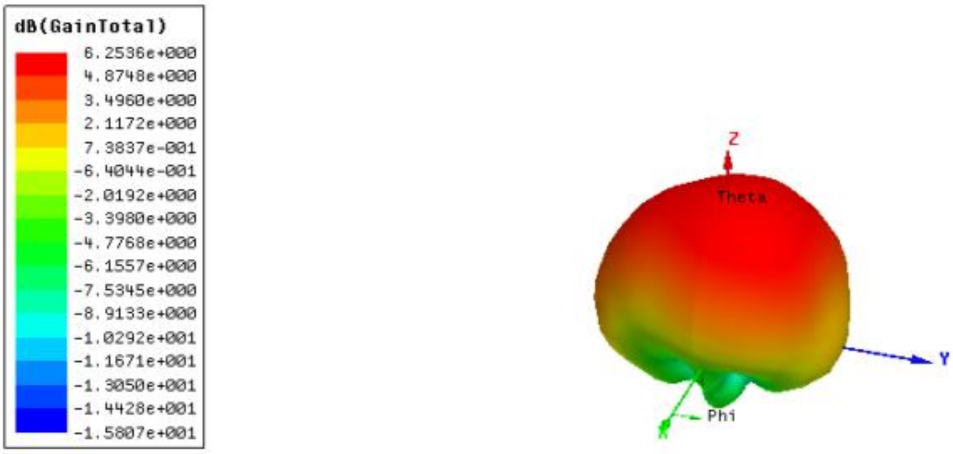

Figure 8. 3D-radiation pattern of antenna

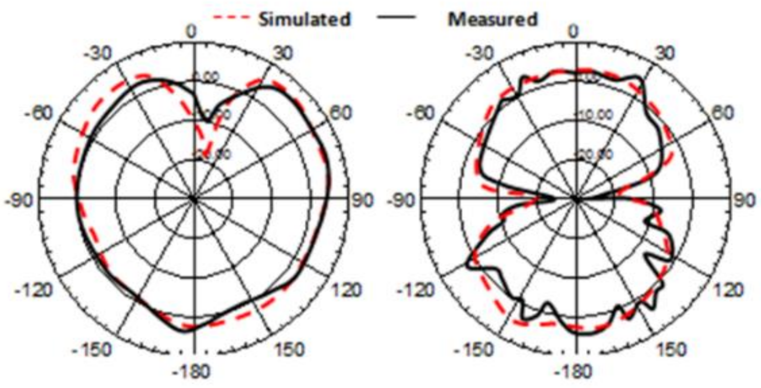

Figure 9. 2D-radiation pattern of antenna at 26 GHz: (a) Phi = 0°; (b) Phi = 90°

5.3. Gain, impedance and VSWR

Figure 10 illustrates the antenna's gain around 6.2 dB at 26 GHz. Additionally, Figure 11 demonstrates a good adaptation of the antenna with real impedance consistently hovering near 50 Ω. Moreover, VSWR < 2, closely associated with the reflection coefficient, indicates the power reflected by an antenna, confirming alignment with the resonant frequency, as depicted in Figure 12.

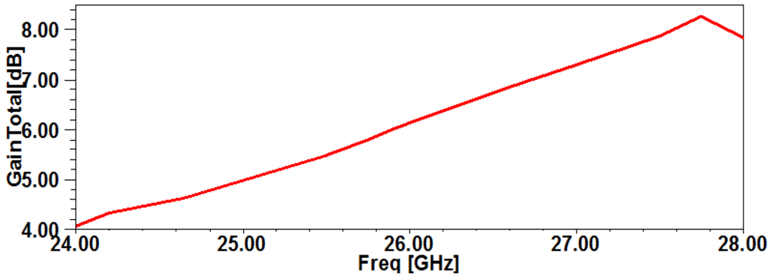

Figure 10. Peak gain of proposed work

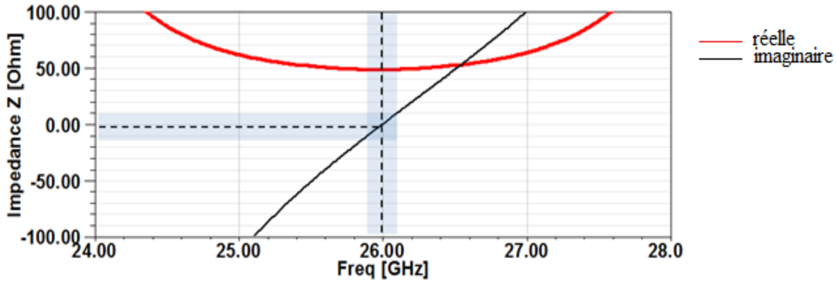

Figure 11. Impedance of patch antenna at 26 GHz

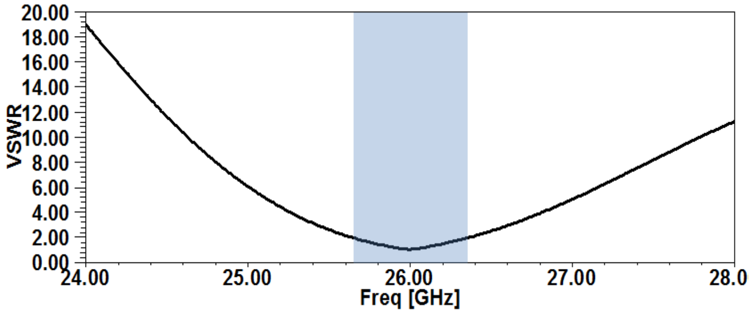

Figure 12. VSWR at 26 GHz

5.4. Conversion circuit

Figure 13 illustrates the design of the series mono-diode conversion circuit for proposed antenna, which includes a Schottky diode of type HSMS-286B, a 60 pF capacitor, and a load resistance of 600 Ω. To enhance the DC voltage value, an adapter circuit is introduced between the generator and the rectification circuit. This adapter circuit minimizes the reflected power value and maximizes the throttle output, comprising a 2.1 nH inductance and a 0.3 pF capacitor. The efficiency of this system can be examined $\eta = \frac{P_{DC}}{P_{RF}}$ with output DC power (P_{DC}), input RF power (P_{RF}), output DC voltage (V_{DC}), and resistive load (R_L).

We will examine the variation of conversion efficiency concerning the input RF power and the load. In Figure 14 (a), the efficiency (%) is plotted against the resistive load (RL) ranging from 100 Ω to 1 KΩ. The maximum efficiency reaches 36% with an optimal load of 300 Ω and an incident power of 10 dBm.

Figure 14 (b) displays the efficiency (%) relative to the input power (dBm). The efficiency peaks at 42.25% for a load resistance of 300 Ω and an input power of 15 dBm.

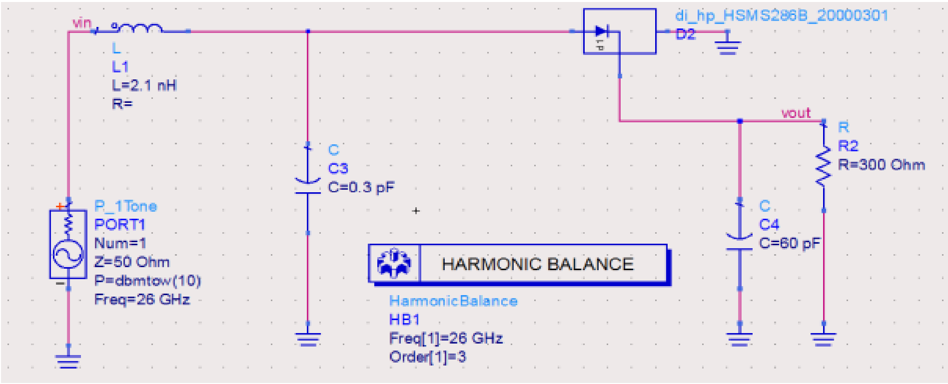

Figure 13. Schema of the conversion circuit

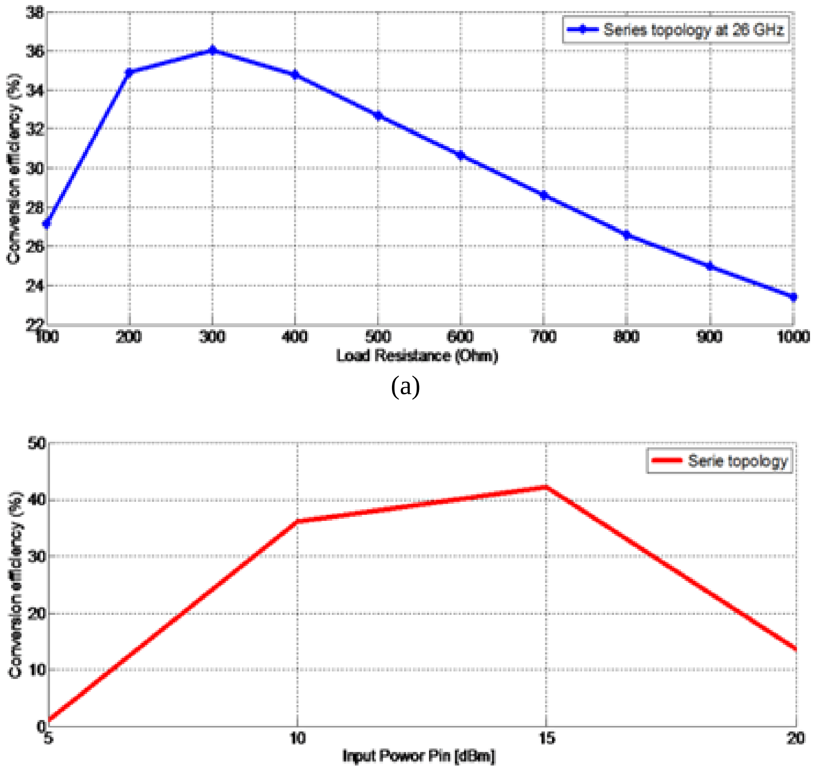

(a)

(b)

Figure 14. Variation of conversion efficiency as a function of (a) resistance, and (b) RF power

5.5. Integration of patch antenna and solar cell

Producing millimeter antennas for 5G represents a major challenge due to the specific requirements of this technology. The design and manufacturing of these antennas requires increased precision and a deep understanding of the properties of millimeter waves. These technical challenges must be overcome to ensure optimal performance and effective coverage of 5G networks. Based on the simulation and measurement results obtained, our research team has effectively developed a 3.5 GHz solar rectenna prototype illustrated in Figure 15. We affirm the substantial advantages of our "solar rectenna" for energy harvesting forthcoming communication systems.

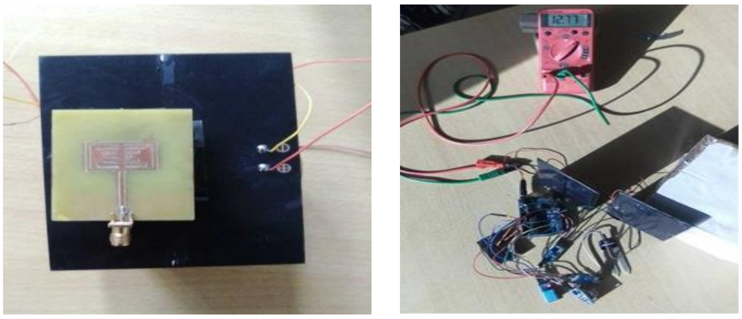

(a) (b)

Figure 15. Prototype of energy-autonomous connected object: (a) the antenna below the solar cell, (b) position of maximum recovered energy

6. CONCLUSION

This paper presents the design and analysis of compact patch antenna tailored for 5G cellular applications, operating at 26 GHz with an impedance bandwidth of 700 MHz. Additionally, the paper explores energy harvesting technology for the IoT environment, providing a sustainable energy source through a solar rectenna. This innovative optical rectenna system harnesses both solar and RF energy, achieving an impressive RF-DC conversion efficiency of approximately 42.25%.

REFERENCES

[1] I. Budhiraja, S. Tyagi, S. Tanwar, N. Kumar, and J. J. P. C. Rodrigues, "Tactile internet for smart communities in 5G: An insight for NOMA-based solutions," *IEEE Transactions on Industrial Informatics*, vol. 15, no. 5, pp. 3104–3112, May 2019, doi: 10.1109/TII.2019.2892763.

[2] R. Gupta, A. Shukla, and S. Tanwar, "AaYusH: A smart contract-based telesurgery system for healthcare 4.0," *2020 IEEE International Conference on Communications Workshops (ICC Workshops)*, Dublin, Ireland, 2020, pp. 1-6, doi: 10.1109/ICCWorkshops49005.2020.9145044.

[3] S. Li, L. Da Xu, and S. Zhao, "5G Internet of Things: A survey," *Journal of Industrial Information Integration*, vol. 10, pp. 1–9, Jun. 2018, doi: 10.1016/j.jii.2018.01.005.

[4] I. F. Akyildiz, S. Nie, S. C. Lin, and M. Chandrasekaran, "5G roadmap: 10 key enabling technologies," *Computer Networks*, vol. 106, pp. 17–48, Sep. 2016, doi: 10.1016/j.comnet.2016.06.010.

[5] M. Agiwal, A. Roy, and N. Saxena, "Next generation 5G wireless networks: A comprehensive survey," *IEEE Communications Surveys and Tutorials*, vol. 18, no. 3, pp. 1617–1655, 2016, doi: 10.1109/COMST.2016.2532458.

[6] A. Gohil, H. Modi, and S. K. Patel, "5G technology of mobile communication: a survey," in *2013 International Conference on Intelligent Systems and Signal Processing (ISSP)*, Mar. 2013, pp. 288–292, doi: 10.1109/ISSP.2013.6526920.

[7] T. S. Rappaport *et al.*, "Millimeter wave mobile communications for 5G cellular: it will work!," *IEEE Access*, vol. 1, pp. 335–349, 2013, doi: 10.1109/ACCESS.2013.2260813.

[8] F. A. Almalki, B. O. Soufiene, S. H. Alsamhi, and H. Sakli, "A low-cost platform for environmental smart farming monitoring system based on IoT and uavs," *Sustainability (Switzerland)*, vol. 13, no. 11, p. 5908, May 2021, doi: 10.3390/su13115908.

[9] C. Bahhar, C. Baccouche, S. Ben Othman, and H. Sakli, "Real-Time intelligent monitoring system based on IoT," in *18th IEEE International Multi-Conference on Systems, Signals and Devices, SSD 2021*, Mar. 2021, pp. 93–96, doi: 10.1109/SSD52085.2021.9429358.

[10] F. A. Almalki, S. Ben Othman, F. A. Almalki, and H. Sakli, "EERP-DPM: energy efficient routing protocol using dual prediction model for healthcare using IoT," *Journal of Healthcare Engineering*, vol. 2021, pp. 1–15, May 2021, doi: 10.1155/2021/9988038.

[11] F. A. Almalki and B. O. Soufiene, "EPPDA: An efficient and privacy-preserving data aggregation scheme with authentication and authorization for IoT-based healthcare applications," *Wireless Communications and Mobile Computing*, vol. 2021, pp. 1–18, Mar. 2021, doi: 10.1155/2021/5594159.

[12] B. O. Soufiene, A. A. Bahattab, A. Trad, and H. Youssef, "PeerP: An priority-based energy-efficient routing protocol for reliable data transmission in healthcare using the IoT," *Procedia Computer Science*, vol. 175, pp. 373–378, 2020, doi: 10.1016/j.procs.2020.07.053.

[13] B. O. Soufiene, A. A. Bahattab, A. Trad, and H. Youssef, "LSDA: Lightweight secure data aggregation scheme in healthcare using IoT," *Proceedings of the 10th International Conference on Information Systems and Technologies*, ICIST '20, Jun. 2020, Art. no. 22, pp. 1–4, doi: 10.1145/3447568.3448530.

[14] W. An, H. Wang, and Y. Luo, "Dual-band antenna integrated with solar cells for WLAN applications," *Frontiers in Physics*, vol. 9, Oct. 2021, doi: 10.3389/fphy.2021.775214.

[15] Y. Luo, J. Lai, N. Yan, W. An, and K. Ma, "Integration of aperture-coupled multipoint feed patch antenna with solar cells operating at dual compressed high-order modes," *IEEE Antennas and Wireless Propagation Letters*, vol. 20, no. 8, pp. 1468–1472, Aug. 2021, doi: 10.1109/LAWP.2021.3087500.

[16] A. Ali, Y. Yun, H. Wang, K. Lee, J. Lee, and I. Park, "Photovoltaic cell with built-in antenna for internet of things applications," *IEEE Access*, vol. 9, pp. 107437–107445, 2021, doi: 10.1109/ACCESS.2021.3101641.

[17] A. Ali, H. Wang, Y. Yun, J. Lee, and I. Park, "Compact slot antenna integrated with a photovoltaic cell," *Journal of Electromagnetic Engineering and Science*, vol. 20, no. 4, pp. 248–253, Oct. 2020, doi: 10.26866/jees.2020.20.4.248.

[18] A. Ali, H. Wang, J. Lee, Y. H. Ahn, and I. Park, "Ultra-low profile solar-cell-integrated antenna with a high form factor," *Scientific Reports*, vol. 11, no. 1, Oct. 2021, doi: 10.1038/s41598-021-00461-w.

[19] B. Naresh, V. K. Singh, and V. K. Sharma, "Integration of RF rectenna with thin film solar cell to power wearable electronics," *International Journal of Microwave and Wireless Technologies*, vol. 13, no. 1, pp. 46–57, Apr. 2021, doi: 10.1017/S1759078720000410.

[20] E. V. V. Cambero, H. P. Da Paz, V. S. Da Silva, H. X. De Araujo, I. R. S. Casella, and C. E. Capovilla, "2.4 GHz coplanar patch antenna with solar cell as radiator for communication and energy harvesting," in *2019 SBMO/IEEE MTT-S International Microwave and Optoelectronics Conference, IMOC 2019*, Nov. 2019, vol. 2019-Jan, doi: 10.1109/IMOC43827.2019.9317682.

[21] S. K. Podilchak, D. Comite, B. K. Montgomery, Y. Li, V. Gomez-Guillamon Buendia, and Y. M. M. Antar, "Solar-panel integrated circularly polarized meshed patch for CubeSats and other small satellites," *IEEE Access*, vol. 7, pp. 96560–96566, 2019, doi: 10.1109/ACCESS.2019.2928993.

[22] Z. Zhang, B. Bai, X. Li, Y. Liu, C. Sun, and Y. Zhang, "Integration of circularly polarized microstrip slot array antenna with amorphous silicon solar cells," *IEEE Antennas and Wireless Propagation Letters*, vol. 19, no. 12, pp. 2320–2323, Dec. 2020, doi: 10.1109/LAWP.2020.3031608.

[23] C. Wang, M. Pang, D. Zhong, Y. Cui, and W. Wang, "A MmWave communication testbed based on IEEE 802.11ad with scalable PtMP configuration," *China Communications*, vol. 19, no. 4, pp. 44–56, Apr. 2022, doi: 10.23919/JCC.2022.04.004.

[24] Y. Kawamoto, H. Nishiyama, N. Kato, S. Yamamoto, N. Yoshimura, and N. Kadowaki, "On real-time data gathering in next generation satellite-routed sensor system (SRSS)," Oct. 2012, doi: 10.1109/WCSP.2012.6542956.

[25] C. Wang, D. Deng, L. Xu, and W. Wang, "Resource scheduling based on deep reinforcement learning in UAV assisted emergency communication networks," *IEEE Transactions on Communications*, vol. 70, no. 6, pp. 3834–3848, Jun. 2022, doi: 10.1109/TCOMM.2022.3170458.

[26] D. Deng, C. Wang, M. Pang, and W. Wang, "Dynamic resource allocation with deep reinforcement learning in multibeam satellite communication," *IEEE Wireless Communications Letters*, vol. 12, no. 1, pp. 75–79, Jan. 2022, doi: 10.1109/LWC.2022.3217316.

[27] W. C. Brown, "Performance characteristics of the thin-film, etched-circuit rectenna," in *IEEE MTT-S International Microwave Symposium Digest*, 1984, pp. 365–367, doi: 10.1109/mwsym.1984.1131793.

[28] P. C. Kar and M. A. Islam, "Design and performance analysis of a rectenna system for charging a mobile phone from ambient EM waves," *Heliyon*, vol. 9, no. 3, p. e13964, Mar. 2023, doi: 10.1016/j.heliyon.2023.e13964.

BIOGRAPHIES OF AUTHORS

Chokri Baccouch was born in Gabes Tunisia, in 1988. Assistant professor at Paris 8 University. He received PhD in telecommunications from the National School of Engineering of Tunis (ENIT), Tunisia in 2018. He received the National diploma in engineering telecommunications and networks from the National School of Engineering of Gabes (ENIG), Tunisia, in 2012. His research works in IoT, artificial intelligence, communications systems, and harvesting energy. He can be contacted at email: chokri.baccouch13@gmail.com.

Saleh Omar was born in Ajdabya, Libya, in 1983. He received master in telecommunications engineering from UTHM, Malaysia in 2013. He is working PhD student at National Engineering School of Gabes (ENIG) Tunisia. His research works in FSS, and antenna design for communications systems. He can be contacted at email: saleheltapony911@gmail.com.

Belgacem C. Rhaimi is an associate professor in computer sciences and information engineering (CSIE). He joined the National Engineering High School at Gabes named (ENIG) where he is actually employed since September 1991. After a doctorate thesis earned at the National Engineering High School at Tunis (ENIT), he received the Ph.D. degree from ENIG, University of Gabes, Tunisia in 1992. He is a member of the Research Laboratory MACS at ENIG as activities supervisor dealing with signal processing and communications research field. Currently, his research areas cover signal processing and mobile communications. He is currently working with the University of Gabes. His research interests include information and signal processing, and communications engineering. He can be contacted at email: abouahmed17@gmail.com.